Dalton Transactions

ROYAL SOCIETY OF CHEMISTRY

PAPER

View Article Online
View Journal | View Issue

Cite this: *Dalton Trans.*, 2026, **55**, 3287

Design of water-soluble lanthanide luminescent probes for the selective detection of HOCl

Lucile Bridou,[a] Adam Nhari,[b,c] Loeza Collobert,[d] Dina Akl,[a] Salauat R. Kiraev,[a] Kyangwi Patrick Malikidogo,†[b] Jennifer K. Molloy,[c] Boris Le Guennic,[e] Maryline Beyler,[d] Raphaël Tripier,[d] Olivier Maury *[a] and Olivier Sénèque *[b]

Received 26th November 2025,
Accepted 9th January 2026

DOI: 10.1039/d5dt02832a

rsc.li/dalton

The synthesis and photophysical properties of tacn- or pyclen-based macrocyclic complexes featuring extended thioanisole-picolinate antennas are reported. These systems efficiently sensitize Eu(III) luminescence, whereas Tb(III) emission is quenched due to back-energy transfer (BET). In all lanthanide-containing complexes (Eu, Tb and Gd), the sulfide donor group was readily oxidized by HOCl to the corresponding sulfoxide or sulfone. Upon oxidation, the Tb(III) complexes became highly luminescent and act as OFF–ON probes when excited at the isosbestic point (302 nm). Finally, a water/buffer soluble Tb(III) complex combining ether and sulfide antenna was prepared, exhibiting remarkable sensitivity and selectivity towards HOCl detection.

Introduction

Hypochlorous acid (HOCl), the active species in household bleach, is a powerful disinfectant. It is a weak acid with a pK_a of 7.54 at 25 °C and its conjugate base is hypochlorite (ClO^-).[1] HOCl is a strong oxidant that reacts with a wide variety of biomolecules including amino acids, nucleic acids, protein cofactors such as NAD^+ and unsaturated lipids.[2,3] Among amino acids, sulfur-containing residues such as cysteine and methionine are the primary targets, although lysine and other aromatic residues, *i.e.* tryptophan, tyrosine, phenylalanine and histidine, are also affected. Cysteine, featuring a –SH end-group, can undergo oxidative dimerization to form disulfide or can be oxygenated to form sulfenates (RSO^-), sulfinates (RSO_2^-), and sulfonates (RSO_3^-). In contrast, methionine, featuring an –SMe end-group, can be oxidized into sulfoxide (RS(O)Me) and sulfone ($RS(O)_2Me$). Lysine reacts through its side-chain amino group to form chloramine, another potent oxidizing agent. Aromatic side chains of amino acids can undergo chlorination and other biological targets, including nucleobases, co-factors and lipids, also form chlorinated products. HOCl plays a crucial role in the innate immune response, being produced in large amounts within the phagosomes of macrophages and neutrophils by myeloperoxidases from H_2O_2 and Cl^-.[4] At lower concentrations, HOCl has also been proposed to act as a mediator in biological signaling.[5]

The biological significance of HOCl has motivated the development of fluorescent probes for its detection. Most reported systems rely on organic fluorophores, whose emission is modulated by the presence of HOCl, typically through an irreversible chemical transformation (activity-based probes).[6–8] Several mechanisms have been exploited for the selective detection of HOCl, including the oxidation of phenols to quinones, oximes to aldehydes, alkenes to aldehydes and sulfides to sulfoxides or sulfones.

Luminescent lanthanide(III) (Ln(III)) complexes are attractive alternatives to organic fluorophores for biological applications.[9] They exhibit sharp emission bands at fixed wavelengths, characteristic of each lanthanide, and are largely independent of the surrounding environment. Moreover, they possess long-lived emission lifetimes in the microsecond-to-millisecond range. These properties make them easy to distinguish from the endogenous organic fluorescence of biological systems, which is characterized by broad emission bands and short-lived signals (in the nanosecond range).[10] Because f–f transitions are Laporte forbidden, efficient sensitization of Ln(III) complexes relies on the antenna effect.[11] A light-harvesting chromophore, referred to as an antenna, is positioned in close proximity to the Ln(III) center. Upon photon absorption, the antenna transfers its

[a]*CNRS UMR 5182, Laboratoire de Chimie, Univ Lyon, ENS de Lyon, F-69007 Lyon, France. E-mail: olivier.maury@ens-lyon.fr*
[b]*Univ. Grenoble Alpes, CNRS, CEA, IRIG, LCBM (UMR 5249), F-38000 Grenoble, France. E-mail: olivier.seneque@cnrs.fr*
[c]*Univ. Grenoble Alpes, CNRS, DCM (UMR 5250), F-38000 Grenoble, France*
[d]*Univ Brest, UMR CNRS 6521 CEMCA, 6 avenue Victor le Gorgeu, F-29200 Brest, France*
[e]*Univ Rennes, CNRS, ISCR (Institut des Sciences Chimiques de Rennes) UMR 6226, F-35000 Rennes, France*
† Present address: Faculté des Sciences et Technologies, Université de Goma, B. P. 204 Goma, R. D. Congo.

energy to the Ln(III), thereby populating its emissive excited state. For a given Ln(III) ion, the antenna must be carefully selected: the donor state, most often the first triplet excited state, should lie approximately 2000–5000 cm^{-1} above the Ln(III) emissive excited state to ensure efficient energy transfer while preventing back-energy transfer (BET).[12,13] Compared with organic-fluorophores, Ln-based HOCl-responsive probes are still rare.[9,14,15] Most reported examples come from the group of Yuan. One strategy for designing HOCl-responsive Ln(III) complexes employed an aminophenyl-functionalized antenna, which quenched the excited chromophore, likely *via* photoinduced electron transfer, thereby blocking the Ln(III) sensitization.[16–19] Upon reaction with HOCl, the quenching moiety is cleaved, restoring efficient Ln(III) sensitization, and thereby switching on the Eu(III) emission. Another strategy used a Eu(III) complex bearing two β-diketonate ligands that are oxidized by HOCl. This oxidation releases Eu(III), quenching its emission.[20,21] These probes were used for HOCl imaging in cells by time-gated microscopy with UV excitation (λ_{ex} = 330–380 nm). Sørensen and coworkers also reported Ln(III) complexes (Ln = Tb or Eu) incorporating a proximal hydroquinone, where reaction with HOCl altered the Ln(III) emission, although the underlying mechanism was not determined.[22]

Over the past decade, many groups focused on developing luminescent lanthanide bioprobes for microscopy imaging. A major drawback of visible-emitting Ln(III) complexes is their reliance on UV excitation for luminescence sensitization, which can damage biological samples. For this reason, current commercial microscopes are not equipped with such high-energy light sources. This limitation can be overcome by using two-photon (2P) absorbing antennas, which shift the excitation wavelength from the UV to the red/near-infrared region, significantly less damaging for *in vivo* studies.[23–25]

We have recently reported **LnL$_1$** complexes (Ln = Eu, Tb, Gd) that comprise a triazacyclononane (tacn) macrocycle bearing three picolinate groups extended with a thioanisolyl moiety (Chart 1).[26] The 2P-absorbing 4-(4-methylthiophenyl)picolinate antenna efficiently sensitizes the luminescence of Eu(III) but not that of Tb(III). As mentioned above, sulfides readily react rapidly with HOCl to yield sulfoxides and other poly-oxygenated derivatives.[2,27,28] Oxygenation of the 4-(4-methylthiophenyl)picolinate antenna is therefore expected to alter its sensitizing properties. In this study, we first examined the luminescence response of the **LnL$_1$** and **LnL$_2$** complexes shown in Chart 1 to assess their potential as HOCl-sensitive probes. Building on the limitations identified for these two complexes, namely poor water solubility and a blue-shift in absorption upon oxidation, we then designed and evaluated an improved structure, **TbL$_3$**, as a HOCl-responsive probe potentially suitable for 2P-microscopy imaging.

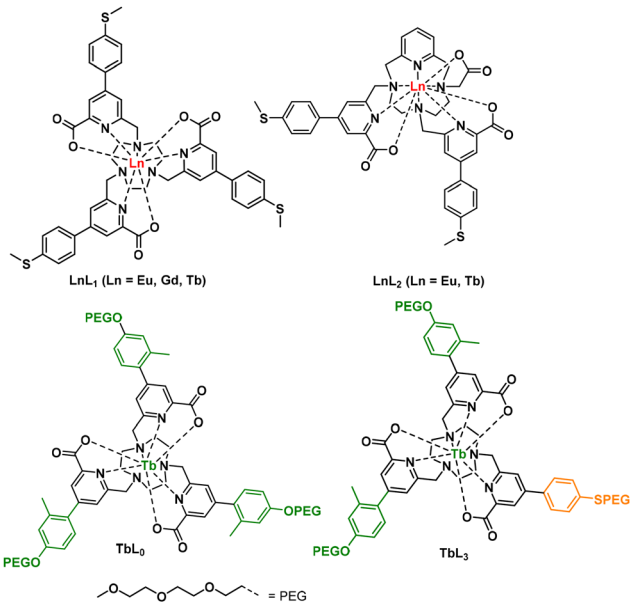

Chart 1 Structures of the discussed and studied Ln(III) complexes.

Results and discussion

Synthesis

The syntheses and characterization of the **EuL$_1$**, **TbL$_1$** and **GdL$_1$** complexes based on tacn macrocyclic ligands bearing three thioanisolyl antennas have been described recently.[26] The pyclen derivatives **LnL$_2$** have been prepared according to reported procedures[24] but using the thioanisolyl picolinate antenna. The synthesis of **L$_2$** is based on the key compound **1** (Scheme 1), described earlier,[29,30] which consists of a pyclen macrocycle, regiospecifically *N*-functionalized at a lateral position with an acetate pendant arm. The pyclen derivative **1** was reacted with mesylated thioanisolyl antenna **2** in acetonitrile with potassium carbonate under reflux for 24 h. As the reaction proceeded slowly, an additional amount of activated antenna **2** was added, and the mixture was refluxed for further 24 h to drive the conversion. After cooling, the reaction mixture was filtered, evaporated, and purified on an alumina column, affording the ligand precursor **L$_2$′** in 48% yield. The methyl ester-protected precursor **L$_2$′** was then dissolved in a THF : MeOH 4 : 1 mixture and saponified with potassium hydroxide under stirring at 70 °C for 16 h. After solvent removal, and elimination of salts by centrifugation, the product was subjected to dialysis, yielding compound **L$_2$** as a white powder in quantitative yield. The final lanthanide complexes were prepared by dissolving **L$_2$** in water, adjusting the pH to 6.3–6.4 with HCl or KOH and adding 1.1 equiv. of the corresponding europium and terbium chloride hexahydrate salts. The reaction mixtures were stirred for 48 h under reflux (Ln = Eu) or at r.t. (Ln = Tb), then centrifuged and purified by C_{18} reverse-phase flash chromatography with a H_2O : MeCN gradient. The complexes were isolated as white solids with yields depending on the lanthanide ion and reaction conditions (85% for **EuL$_2$** and 10% for **TbL$_2$**).

The water soluble tacn-based **TbL$_3$** complex featuring two distinct antennas has been prepared through a multistep synthesis (Scheme 2). The thioanisolyl picolinate antenna **A$_2$** was first synthesized from the polyethyleneglycol (PEG) functiona-

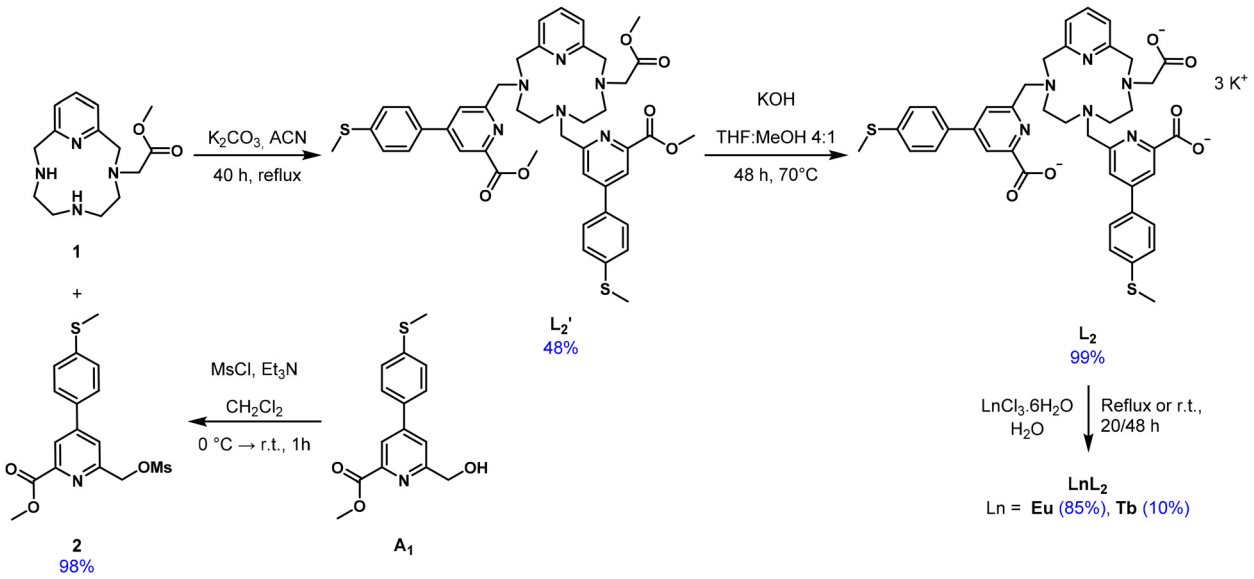

Scheme 1 Synthesis of pyclen-based ligand L_2 and LnL_2 complexes (Ln = Eu, Tb).

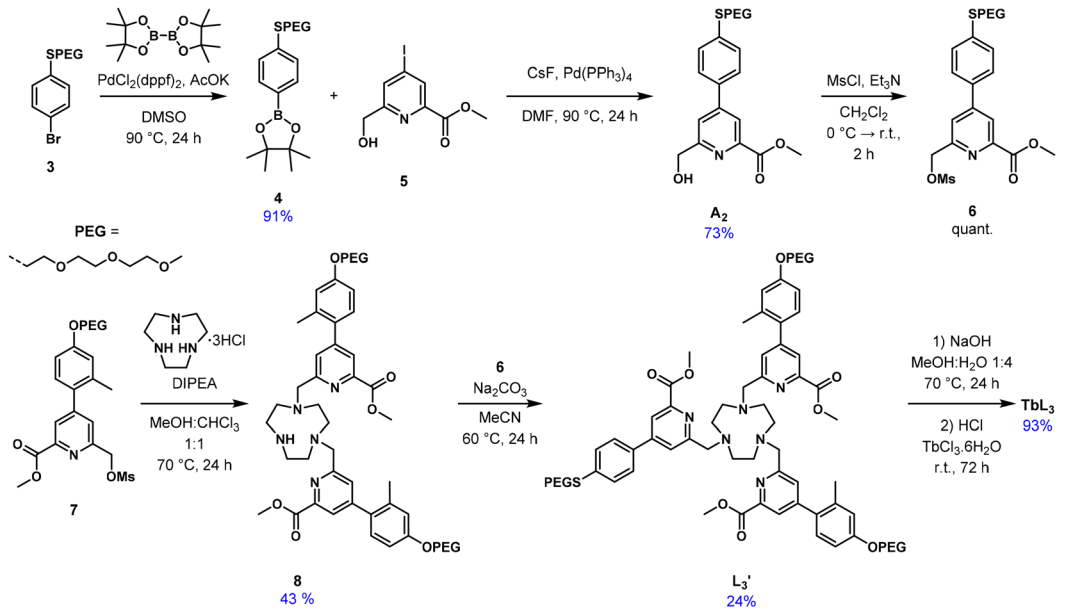

Scheme 2 Synthesis of SPEG-functionalized antenna A_2, ligand precursor L_3' and the TbL_3 complex.

lized 4-bromothioanisole **3**.[31] Miyaura borylation of **3** with bis(pinacolato)diboron afforded the boronic ester **4** in 91% yield which was subsequently employed in a Suzuki–Miyaura coupling with the methyl ester of 6-(hydroxymethyl)-4-iodopicolinate **5**, affording the target SPEG-functionalized antenna $\mathbf{A_2}$ in 73% yield. Alcohol $\mathbf{A_2}$ was then quantitatively converted to the mesylate **6**, suitable for tacn alkylation (*vide infra*). Alternatively, antenna $\mathbf{A_2}$ could be obtained *via* a similar Suzuki reaction with dimethyl *p*-iododipicolinate followed by monoreduction of a resulting diester $\mathbf{A_2}'$ to the alcohol $\mathbf{A_2}$ with sodium borohydride (Scheme S1 in the SI). However, this route resulted in a significantly lower yield (34% *vs.* 73%) due to competitive reduction of both methyl esters in $\mathbf{A_2}'$ yielding undesired bis-alcohol byproducts. The second antenna with the twisted charge-transfer character, was proved to sensitize bright Tb(III) emission in a tacn-trispicolinate macrocyclic environment with a 74% quantum yield in water.[32] The mesylate of the twisted antenna **7** was used for the bis-alkylation of tacn in the presence of Hünig's base in a 1 : 1 dry MeOH : $CHCl_3$ mixture under reflux for 24 h. Using a strict 1 : 2 stoichiometric ratio of tacn to activate antenna **7** and a weaker organic base instead of alkali carbonates allowed the for-

mation of bis-alkylated tacn derivative **8**, which was purified *via* column chromatography on neutral alumina (43%). The remaining secondary amine of the bis-alkylate **8** was reacted with the mesylate of the SPEG-functionalized antenna **6** using sodium carbonate as a base in dry acetonitrile upon heating to 60 °C for 24 h. The formed [2 + 1] ligand precursor $\mathbf{L_3}'$ required identical chromatographic purification as in the previous step, affording the target molecule in diminished yield (24%). The protected ligand $\mathbf{L_3}'$ was saponified with sodium hydroxide in a methanolic-aqueous 1 : 4 mixture at 70 °C for 24 h and then reacted *in situ* with terbium chloride after methanol removal and pH adjustment to 6.0 with HCl and NaOH. Complexation was performed at r.t. over 72 h. $\mathbf{TbL_3}$ was isolated as a colorless solid in 93% yield after extraction with dichloromethane.

Oxidation of the thioanisolyl antenna

The oxidation of the $\mathbf{A_1}$ sulfide functional group to sulfoxide and sulfone moieties by HOCl was studied using UV-Vis absorption spectroscopy and high-resolution mass spectrometry (HRMS). The thioanisolyl antenna $\mathbf{A_1}$ experienced a rapid reaction of the sulfide function upon treatment with 3 equiv. of HOCl in MeOH (C = 0.1 mM) as evidenced by the pronounced blue shift of the UV-Vis absorption transition of the charge-transfer (CT) band from λ_{abs} = 312 nm of $\mathbf{A_1}$ to 270 nm

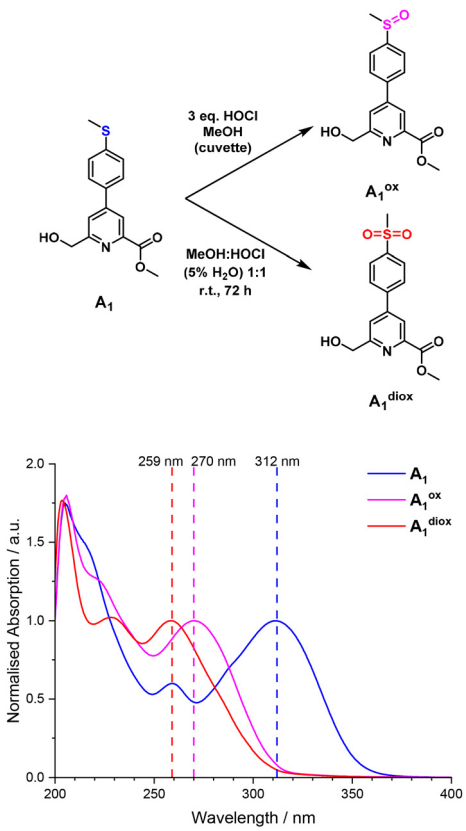

Fig. 1 (Top) Oxidation of antenna $\mathbf{A_1}$ to $\mathbf{A_1}^{ox}$ and $\mathbf{A_1}^{diox}$ by HOCl. (Bottom) UV-Vis absorption spectra of antenna $\mathbf{A_1}$ in MeOH before and after HOCl oxidations (C = 0.1 mM).

of $\mathbf{A_1}^{ox}$ (Fig. 1). HRMS analysis of the cuvette titration products confirmed the formation of the mono-oxidized sulfoxide $\mathbf{A_1}^{ox}$ (Fig. S1, m/z $[M + H]^+$ = 306.0795 for $C_{15}H_{16}NO_4S$ along with the corresponding sodium adduct). The reaction kinetics of the mono-oxidized product is very fast, and in our hands, the reaction was completed within the mixing time.[27,33] The over-oxidized sulfone $\mathbf{A_1}^{diox}$ was also detected (m/z $[M + Na]^+$ = 344.0562 for $C_{15}H_{15}NNaO_5S$). To characterize the fully oxidized product of $\mathbf{A_1}$, an *in situ* oxidation was carried out by stirring 0.028 mmol of $\mathbf{A_1}$ (C = 10 mM) a 1 : 1 MeOH : HOCl (5% aqueous solution mixture) at r.t. for a longer time, *i.e.* 72 h, to ensure complete formation of the end-product. The isolated product of the oxidation was $\mathbf{A_1}^{diox}$, showing a further blue-shifted absorption maximum at λ_{abs} = 259 nm (Fig. 1). HRMS data confirmed the quantitative conversion to the sulfone product (Fig. S2, m/z $[M + H]^+$ = 322.0742 for $C_{15}H_{16}NO_5S$ and the corresponding sodium adduct). In the ^{1}H NMR spectrum, the di-oxidized species $\mathbf{A_1}^{diox}$ were characterized by a deshielded methyl signal (3.11 ppm), shifted by almost 0.6 ppm compared to the sulfide precursor.[4] The pyridine and other aliphatic protons remained largely unaffected, while the aromatic signals of the phenyl ring conjugated to the sulfone group appeared ~0.5 ppm downfield, consistent with reduced electron density at the sulfur in the +6 oxidation state (Fig. S3).

To rationalize the experimentally observed hypsochromic shift of the lowest-energy charge-transfer band upon stepwise oxidation of antenna $\mathbf{A_1}$, we performed a theoretical study based on Time-Dependent Density Functional Theory (TD-DFT, see the SI for computational details). The calculated transitions were consistently red-shifted by about 12–24 nm relative to the experiment (Table S1). Nevertheless, the difference between $\mathbf{A_1}$ and $\mathbf{A_1}^{ox}$ in the theoretical absorption maxima of the most red-shifted bands matched the experimental value, *i.e.* 42 nm (λ_{abs} = 336 nm and 294 nm for $\mathbf{A_1}$ and $\mathbf{A_1}^{ox}$, respectively). According to the calculations, the sulfone derivative $\mathbf{A_1}^{diox}$ exhibited an absorption transition at λ_{abs} = 271 nm, which represents a 23 nm blue-shift compared to $\mathbf{A_1}^{ox}$. This shift was somewhat larger than the experimental value ($\Delta\lambda_{abs}$ = 11 nm). The nature of the transitions was found to be predominantly HOMO → LUMO in $\mathbf{A_1}$ (98.3%) and to a slightly lesser extent in the sulfoxide form (93.3%). By contrast, the charge-transfer character was markedly reduced in the sulfone form (78.2%, Tables S1 and S2). This trend was also reflected in the molecular orbital representations: in the di-oxidized antenna $\mathbf{A_1}^{diox}$, the majority of the electron density is no longer localized around the sulfur atom, thereby hindering effective charge transfer from the donor (methylphenylsulfone) to the acceptor (picolinate) moieties of the molecule (Fig. S4–S6).

Responsive lanthanide complexes

Comparable HOCl oxidation studies were carried out on representative examples of both lanthanide complex families $\mathbf{LnL_1}$ and $\mathbf{LnL_2}$ (Ln = Eu, Gd, Tb) featuring three and two thioanisolyl moieties, respectively. In HRMS, the major peaks corresponded to the addition of three oxygen atoms in the case of the tacn-based complexes and two oxygen atoms in the case of

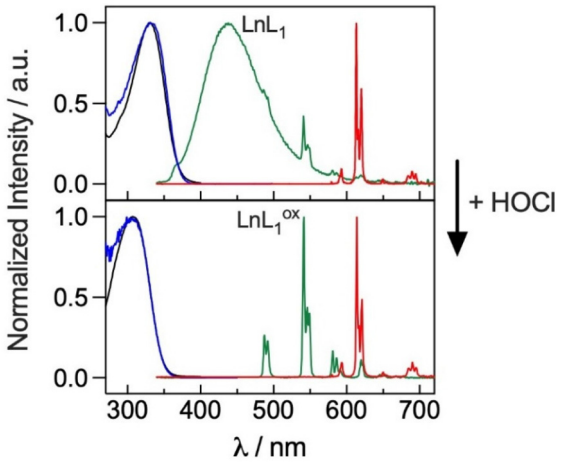

Fig. 2 Absorption (black), excitation (blue, λ_{em} = 614 nm for Eu and 541 nm for Tb) and steady-state emission spectra of **LnL$_1$** (Ln = Tb, green; Ln = Eu, red) in methanol solutions at 293 K before (top, λ_{ex} = 330 nm) and after (bottom, λ_{ex} = 283 nm) addition of excess HOCl.

the pyclen-based complexes (Fig. S7–S11). Together with the short time between HOCl addition and analysis, this suggests that sulfoxide is formed first on each antenna (sulfone would require a longer reaction time, *vide supra*). In both the tacn- and pyclen-based systems, **TbL$_1^{ox}$** and **EuL$_2^{ox}$**, minor amounts of over-oxidized species were also detected, namely sulfone/sulfoxide or bis-sulfone derivatives.

The photophysical properties of **EuL$_1$** and **TbL$_1$** in diluted MeOH solutions have been reported previously (Fig. 2 and Table 1).[26] Their absorption spectra show an Intra-Ligand Charge Transfer (ILCT) transition from the electron-donating thioanisolyl moieties to the electron-withdrawing pyridine group with a maximum at 330 nm. The **EuL$_1$** complex showed a long excited-state lifetime (1 ms), high quantum yield (44%) and strong brightness (25 000 M^{-1} cm^{-1}), making it particularly attractive for both 1P- and 2P-luminescence applications.[26] In contrast, **TbL$_1$** exhibited poor emissive properties, dominated by ligand-centered fluorescence, with only a weak Tb(III) emission signal detectable in the red tail of the fluorescence emission. This weak Tb(III) emission was attributed to inefficient sensitization of Tb(III) by the thioanisolyl antenna, caused by an efficient back-energy transfer (BET) from the Tb(III) $^5D_4$ excited state (20 500 cm^{-1}) to the triplet associated with the thioanisolyl antenna (20 600 cm^{-1}). The small energy gap between these states (~100 cm^{-1}) was estimated using the corresponding **GdL$_1$** complex to determine the position of the ligand triplet excited state (Fig. 3a).

The photophysical properties of the thioanisolyl antenna complexes changed drastically upon addition of excess HOCl. First, the ILCT transition was blue-shifted by 42 nm. This shift reflected oxidation of the thioether fragment, which suppressed its donor character and thereby reduced the ILCT contribution to the absorption band (*vide supra*). Second, the luminescence properties of the **EuL$_1^{ox}$** complex were essentially unchanged with identical lifetime and emission profile, indicating that the oxidized antenna still efficiently sensitized Eu(III) and that the coordination sphere of the central ion was preserved. In contrast, the photophysical behavior of **TbL$_1^{ox}$** was profoundly different. The ligand-centered transition disappeared completely, while an intense Tb(III) emission pattern emerged, accompanied by an increased luminescence lifetime of 1.29 ms. This indicated that the oxidized antenna was now able to efficiently sensitize Tb(III).

To rationalize the strong enhancement of 4f–4f luminescence, the position of the oxidized ligand triplet state was determined using the **GdL$_1^{ox}$** complex *via* low temperature time-gated emission spectroscopy. The long-lived triplet emission of **GdL$_1^{ox}$** was significantly blue-shifted to 442 nm compared to 485 nm for **GdL$_1$**, corresponding to a higher-energy triplet excited state at 22 600 cm^{-1} (Fig. 3a). The resulting larger energy gap between this triplet and the Tb(III) accepting level (2100 cm^{-1}) effectively suppressed BET and eliminated triplet-mediated oxygen quenching (Fig. 3b). Consequently, **TbL$_1^{ox}$** became strongly luminescent owing to the removal of this major non-radiative deexcitation pathway.

Similar results were obtained with the pyclen-based **EuL$_2$** and **TbL$_2$** complexes as the same antenna was involved in the Ln(III) luminescence sensitization process (Table 1 and Fig. S12). While **EuL$_2$** and **EuL$_2^{ox}$** exhibited similar luminescence properties, only the oxidized form of the antenna efficiently sensitizes the Tb(III) emission in **TbL$_2^{ox}$**. The photophysical properties of the complexes were therefore governed primarily by the nature of the antenna, the macrocycle exerting a marginal influence. These findings highlight both series of complexes as promising candidates for sensing applications, which motivated the subsequent titration experiments.

Table 1 Photophysical properties of **LnL$_1$** and **LnL$_2$** complexes (Ln = Tb and Eu) in methanol and **TbL$_3$** in PBS buffer (pH 7.4) in the absence or in the presence of an HOCl excess

	Initial complexes[a]		After addition of HOCl[b]		
Complex (solvent)	λ_{max}^{abs} (nm) (ε, M^{-1} cm^{-1})	Φ (%) (τ, ms)	λ_{max}^{abs} (nm)	τ (ms)	Titration I_F/I_0@λ_{ex} (nm)
TbL$_1$ (MeOH)	330 (53 000)	1.6 (<0.02)	281	1.29	×36@301
EuL$_1$ (MeOH)	330 (53 000)	44 (0.98)	281	1.03	÷420@370
TbL$_2$ (MeOH)	328 (45 000)	0.9 (<0.02)	279	1.54	×406@302
EuL$_2$ (MeOH)	329 (45 000)	46 (1.33)	279	1.34	÷730@370
TbL$_3$ (PBS)	305 (31 000)	4.6[c] (<0.02)	282	1.13	×15@298

[a] λ_{ex} = 330 nm, precision for ε = ±10%. [b] λ_{ex} = 283 nm. [c] 2.9% for Tb emission only.

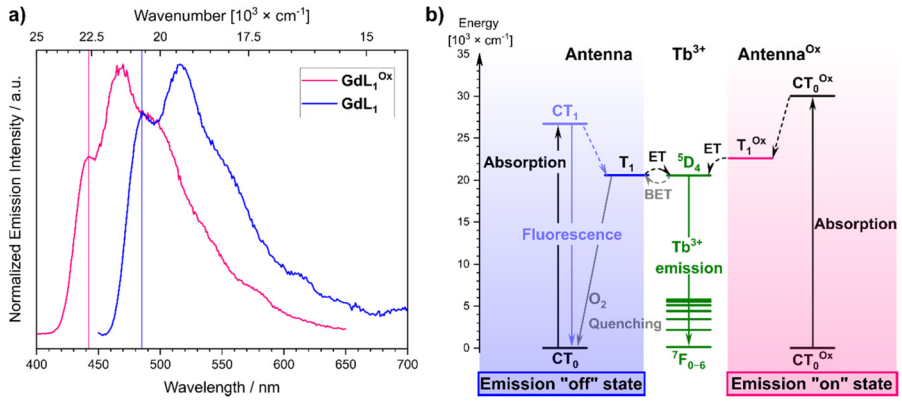

Fig. 3 (a) Time-gated emission spectra (delay = 50 μs) in a methanol : ethanol 1 : 4 mixture at 77 K of $\mathbf{GdL_1}$ before (blue, λ_{ex} = 330 nm) and after (pink, λ_{ex} = 290 nm) addition of an excess of HOCl; the coloured lines indicate the energy position of the triplet state. (b) Perrin-Jablonski diagram of the Tb(III) luminescence sensitisation in $\mathbf{LnL_{1-3}}$ complexes before and after oxidation by HOCl. CT = charge transfer state, ET = energy transfer, BET = back energy transfer, T_1 = first triplet excited state.

Titration experiments

The titration experiments of $\mathbf{EuL_1}$, $\mathbf{TbL_1}$, $\mathbf{EuL_2}$ and $\mathbf{TbL_2}$ were carried out in diluted methanol solutions [Optical Density (OD) was 0.2–0.4] by successive addition of HOCl equivalents directly into a 1 cm spectroscopic cuvette. The results are reported in Fig. 4, 5, S13 and S14, respectively. The reaction with HOCl was instantaneous; hence, absorption and emission spectra were recorded after each addition. For each titration at a given excitation wavelength (λ_{ex}), the variation of the luminescence intensity at the local emission maxima (λ_{em}) as a function of the number of HOCl equivalents was determined and the total variation of I_F/I_0 (I_0 and I_F representing the initial and final luminescence intensities, Table 1) was measured. In all cases, the absorption spectra clearly showed a single isosbestic point at 302 ± 1 nm indicating an equilibrium between two species: the initial (sulfide) and the oxidized (sulfoxide) antenna. The over-oxidized form (sulfone) detected by mass spectrometry played only a minor role in the titration experiments. The number of HOCl equivalents required for complete titration was estimated to be 15 for $\mathbf{LnL_1}$ and 8 for $\mathbf{LnL_2}$, bearing three and two antennae, respectively. So, *ca.* 4 to 5 equivalents of HOCl per antenna were necessary to fully oxidize all sulfoxide groups. For europium derivatives $\mathbf{EuL_1}$ and $\mathbf{EuL_2}$, both the initial and oxidized forms were emissive. Therefore, luminescence titration was performed at the cut-off wavelength (370 nm) where only the initial form absorbs. Consequently, the decrease in OD at the excitation wavelength (λ_{ex}) accounted for the observed decrease in Eu(III) luminescence. The europium complexes thus behave as emission on–off probes with luminescence intensity divided by factors 420 and 730 between the initial and oxidized forms for $\mathbf{EuL_1}$ and $\mathbf{EuL_2}$, respectively.

The terbium complexes, $\mathbf{TbL_1}$ and $\mathbf{TbL_2}$, were almost non-emissive in their initial state. A luminescence titration was therefore performed by irradiation at the isosbestic point

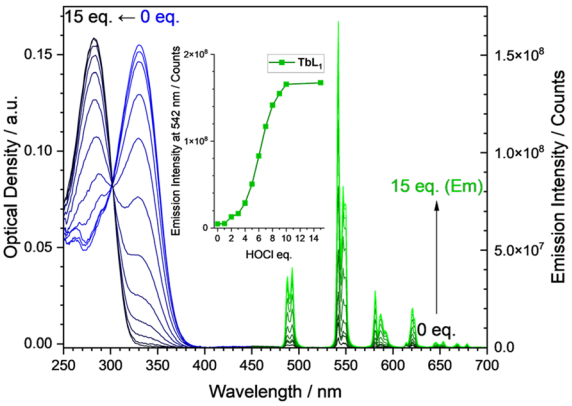

Fig. 5 Titration of $\mathbf{TbL_1}$ by HOCl in MeOH at 293 K: evolution of the absorption spectra (blue to black), evolution of the Tb(III) emission spectra upon 302 nm excitation (black to green), and variation of the 542 nm emission intensity with the number of HOCl equivalents (inset).

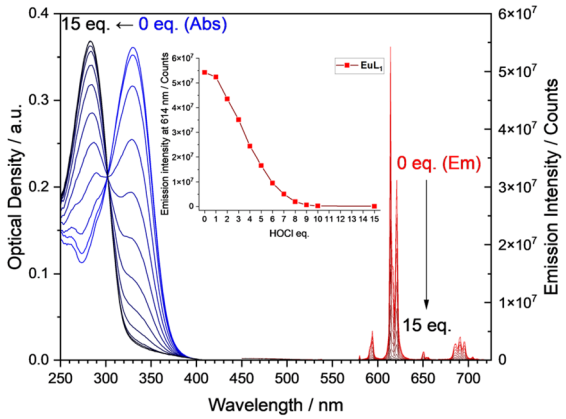

Fig. 4 Titration of $\mathbf{EuL_1}$ by HOCl in MeOH at 293 K: evolution of the absorption spectra (blue to black), evolution of the Eu(III) emission spectra upon 370 nm excitation (red to black), and variation of the 614 nm emission intensity with the number of HOCl equivalents (inset).

where an equal amount of light is absorbed throughout the oxidative photoluminescence titrations (iso-absorption point). Upon oxidation, the $\mathbf{TbL_1}^{ox}$ and $\mathbf{TbL_2}^{ox}$ complexes became strongly emissive, with Tb(III) emission intensities increasing progressively during the titration. The luminescence signal was enhanced by factors of 36 and 406 for $\mathbf{TbL_1}$ and $\mathbf{TbL_2}$, respectively.[34] These complexes thus act as highly sensitive off-on luminescent probes. In conclusion, these titration experiments established a proof-of-concept for this class of complexes as responsive luminescent probes for HOCl detection. The europium derivatives behaved as on–off emission probes upon excitation at 370 nm, while the terbium compounds showed off-on response when irradiated at the isosbestic point (302 ± 1 nm). However, two limitations remain. First, the sulfide antenna does not efficiently sensitize Tb^{3+} luminescence, while the sulfoxide antenna does not absorb above 320 nm. As a result, these probes are unsuitable for 2P microscopy, which requires longer excitation wavelengths (*i.e.* 2P excitation ≥ 690 nm, corresponding to 1P absorption ≥ 345 nm). Second, the $\mathbf{LnL_1}$ and $\mathbf{LnL_2}$ probes are soluble in methanol but not in water, preventing their direct application in biological media.

Water-soluble HOCl probe

To address these drawbacks, complex $\mathbf{TbL_3}$ (Chart 1) was designed featuring two kinds of sensitizing antennae, (4-alkoxy-2-methylphenyl)picolinate and 4-(4-alkylthiophenyl) picolinate, bearing ether and sulfide electron donating groups, respectively. The latter is intended to act as a HOCl-responsive antenna as described above, while the former is expected to remain insensitive to HOCl and provide absorption up to 355 nm. Lanthanide complexes with such an ether-based antenna were previously shown to be suitable for 2P microscopy.[32] The addition of short PEG oligomers ensured the solubility in aqueous solutions of the final Tb(III) complex. $\mathbf{TbL_3}$ was studied in PBS buffer at pH 7.4. Its absorption spectrum exhibits a maximum at 307 nm with a shoulder at *ca.* 285 nm and extends up to 370 nm as expected because of the sulfide-containing antenna. In its initial state, $\mathbf{TbL_3}$ exhibits a modest Tb(III) emission (Φ = 2.9%) and a short Tb(III) emission lifetime (<0.02 ms) along with a residual antenna fluorescence (Φ = 1.7%), similar to what was observed for $\mathbf{TbL_1}$ and $\mathbf{TbL_2}$ (Table 1). However, compared with those complexes, the Tb^{3+} emission is stronger and the Tb(III)/antenna emission ratio is larger (63%), indicating a less efficient quenching by the BET mechanism in the case of $\mathbf{TbL_3}$ due to the presence of a single sulfide antenna. The Tb(III) emission quantum yield of $\mathbf{TbL_3}$ is *ca.* 25 times lower than that of the parent complexes featuring three ether-based antennas (τ = 1.36 ms, Φ = 74% in water).[3] Therefore, a single sulfide antenna is sufficient to effectively quench Tb(III) emission through a BET mechanism in oxygenated water. The excitation spectrum of $\mathbf{TbL_3}$ is blue-shifted compared with the absorption spectrum, indicating weaker Tb(III) sensitization efficiency of the sulfide donor antenna compared with its oxygen-donor counterpart.

$\mathbf{TbL_3}$ was reacted with a 4-fold excess of HOCl in PBS. LC/MS analysis confirmed the complete consumption of $\mathbf{TbL_3}$ and the formation of a new complex, $\mathbf{TbL_3}^{ox}$, showing a +16 mass increase, consistent with the oxidation of the sulfide to a sulfoxide (Fig. S15). The absorption spectrum of $\mathbf{TbL_3}^{ox}$ showed a *ca.* 20 nm blue-shift relative to $\mathbf{TbL_3}$ (Fig. 6) with a maximum at 285 nm and extending up to 355 nm, in line with the reduced CT character of the sulfide donor. Upon oxidation, an intense Tb(III) emission was recovered (Φ = 29%) with a long luminescence lifetime (1.13 ms) and no residual antenna emission (Fig. 6). This behavior is consistent with the suppression of the BET mechanism upon oxidation of the sulfide antenna. Furthermore, the excitation spectrum of $\mathbf{TbL_3}^{ox}$ closely matched its absorption profile, in contrast to $\mathbf{TbL_3}$, indicating that both the ether- and sulfoxide-based antennas efficiently sensitize Tb(III) luminescence.

Then, the titration of $\mathbf{TbL_3}$ with HOCl was performed in PBS at pH 7.4 and monitored by absorption and emission spectroscopy (Fig. S16 and Fig. 7A). In the absorption spectra, the low-energy ILCT band progressively decreased, while a high-energy band emerged, with the evolution directly proportional to the amount of HOCl added. An isosbestic point was observed at 312 nm. Complete oxidation of $\mathbf{TbL_3}$ occurred at *ca.* 1.8 eq. of HOCl. Emission monitoring (λ_{ex} = 298 nm) showed a similar evolution: Tb(III) emission increased proportionally with HOCl concentration up to *ca.* 1.8 eq. beyond which a plateau was reached (Fig. 7A, left). Upon full oxidation, the Tb(III) emission intensity increased 14.7 fold, demonstrating that $\mathbf{TbL_3}$ acts as a turn-off/on probe for HOCl in PBS buffer when excited at *ca.* 300 nm, as observed for the parent probes $\mathbf{TbL_1}$ and $\mathbf{TbL_2}$. To evaluate the role of the (4-alkoxy-2-methylphenyl)picolinate antenna, which absorbs around 350 nm regardless of the redox state, the titration was

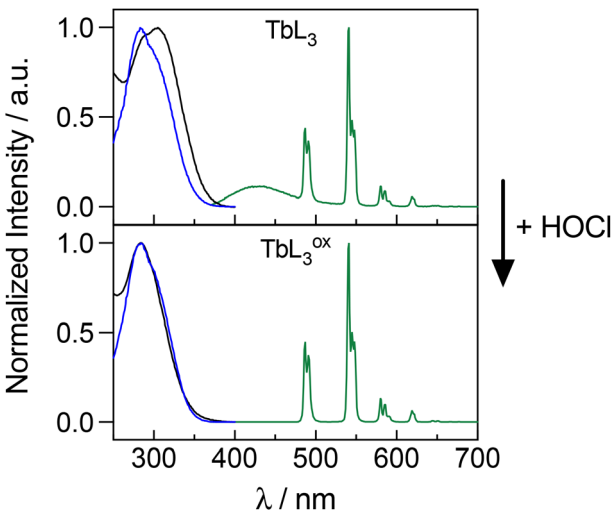

Fig. 6 Absorption (black), excitation (blue, λ_{em} = 541 nm) and steady-state emission spectra of $\mathbf{TbL_3}$ in PBS pH 7.4 at 293 K before (top, λ_{ex} = 298 nm) and after (bottom, λ_{ex} = 298 nm) addition of a 4-fold excess of HOCl.

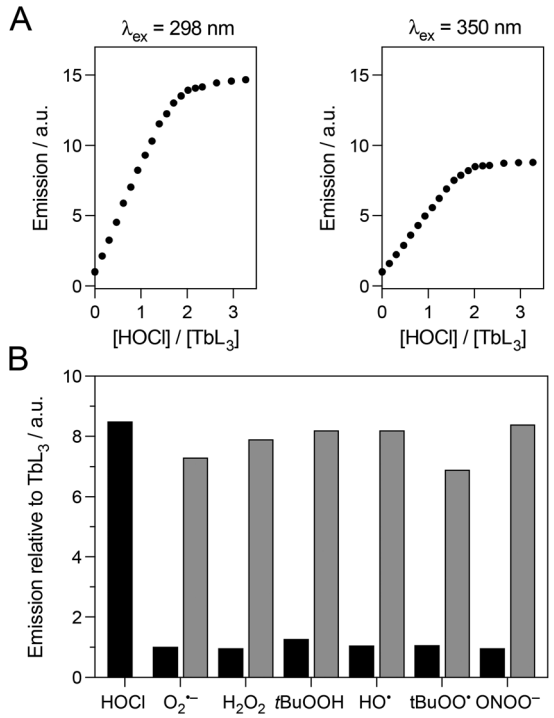

Fig. 7 (A) Evolution of the Tb(III) emission upon titration of $\mathbf{TbL_3}$ by HOCl in PBS pH 7.4 at 293 K under 298 nm (left) and 350 nm excitation (right). Emission (λ_{ex} = 350 nm) of solutions of $\mathbf{TbL_3}$ (5 μM) after addition of 2 eq. of HOCl, $O_2^{\bullet-}$, H_2O_2, *t*BuOOH, $HO^{\bullet}$, *t*BuOO$^{\bullet}$ and $ONOO^-$ (black bars) and after subsequent addition of 10 eq. HOCl (grey bars).

also monitored using the 350 nm excitation wavelength. Interestingly, Tb(III) emission still increased upon HOCl addition when excited at this wavelength (Fig. 7A, right). In this case, an 8.5-fold luminescence enhancement was observed, compared to 14.7-fold under higher-energy excitation (298 nm). This behavior highlights the possibility of using $\mathbf{TbL_3}$ for 2P-microscopy using 700 nm excitation.

Finally, the response of $\mathbf{TbL_3}$ to other oxidizing species ($O_2^{\bullet-}$, H_2O_2, *t*BuOOH, $HO^{\bullet}$, *t*BuOO$^{\bullet}$ and $ONOO^-$) was investigated in PBS at pH 7.4. None of these oxidants produced a significant enhancement of $\mathbf{TbL_3}$ emission, in contrast to HOCl. Moreover, after exposure to these oxidants, $\mathbf{TbL_3}$ remained responsive to HOCl, confirming the absence of interference from competing oxidants in solution (Fig. 7B). Therefore, $\mathbf{TbL_3}$ operates as a highly sensitive and selective off-on responsive probe for HOCl in water, supporting further developments for microscopic applications in HOCl detection.

Conclusion

This work reports the synthesis and photophysical properties of tacn- or pyclen-based macrocyclic complexes featuring an extended thioanisolyl-picolinate antenna. The chromophore efficiently sensitizes Eu(III), whereas Tb(III) emission is quenched by BET to the low-lying triplet state. Oxidation of the sulfide donor group by HOCl yields the corresponding sulfoxide, inducing a blue shift in absorption and a significant increase in the triplet-state energy of the oxidized antenna. Consequently, the oxidized Tb(III) complexes become strongly luminescent. Titration experiments revealed complementary sensing behaviors: Eu(III) complexes behave as ON–OFF probes when excited on the red-tail of the absorption band (370 nm), due to the blue shift upon HOCl oxidation, while Tb(III) complexes act as OFF–ON probes when excited at the isosbestic point (302 nm), reflecting enhanced sensitization by the oxidized antenna. Furthermore, a water or buffer-soluble Tb(III) complex was prepared by combining ether and sulfide antenna, extending the excitation window to 350 nm and making the complex suitable for two-photon microscopy. Reactivity studies toward other oxidants ($O_2^{\bullet-}$, H_2O_2, *t*BuOOH, $HO^{\bullet}$, *t*BuOO$^{\bullet}$ and $ONOO^-$) confirmed its excellent selectivity for HOCl. These results open new avenues for the design of bioconjugated Tb-based bioprobes for *in cellulo* HOCl detection using 2P-microscopy.

Author contributions

Conceptualization: O. S. and O. M.; investigation: L. B., A. N., L. C., D. A., S. R. K., K. P. M., and B. L. G.; validation: O. S., O. M., B. L. G., M. B., R. T., and J. M. K.; writing (original draft): O. M., S. K. R., O. S., and R. T.; writing (review & editing): all authors.

Conflicts of interest

There are no conflicts to declare.

Data availability

The data supporting this article have been included as part of the supplementary information (SI). Supplementary information is available, including detailled synthetic procedures and complete chemical characterizations, photophysical measurement details and computational chemistry results. See DOI: https://doi.org/10.1039/d5dt02832a.

Acknowledgements

The authors acknowledge the Agence Nationale de la Recherche (LANTEN: ANR-21-CE29-0018) for financial support. AN, JKM and OS thank the Labex ARCANE and CBH-EUR-GS (ANR-17-EURE-0003).

References

1 J. C. Morris, *J. Phys. Chem.*, 1966, **70**, 3798–3805.
2 C. C. Winterbourn, in *Encyclopedia of Radicals in Chemistry, Biology and Materials*, Wiley, 2012.

3 M. J. Gray, W.-Y. Wholey and U. Jakob, *Ann. Rev. Microbiol.*, 2013, **67**, 141–160.
4 S. J. Klebanoff, *J. Leukocyte Biol.*, 2005, **77**, 598–625.
5 J. M. Pullar, M. C. M. Vissers and C. C. Winterbourn, *IUBMB Life*, 2000, **50**, 259–266.
6 T. Yudhistira, S. V. Mulay, Y. Kim, M. B. Halle and D. G. Churchill, *Chem. – Asian J.*, 2019, **14**, 3048–3084.
7 D. Wu, L. Chen, Q. Xu, X. Chen and J. Yoon, *Acc. Chem. Res.*, 2019, **52**, 2158–2168.
8 S. Lin, C. Ye, Z. Lin, L. Huang and D. Li, *Talanta*, 2024, **268**, 125264.
9 C. Alexander, Z. Guo, P. B. Glover, S. Faulkner and Z. Pikramenou, *Chem. Rev.*, 2025, **125**, 2269–2370.
10 J.-C. G. Bünzli and S. V. Eliseeva, in *Lanthanide Luminescence: Photophysical, Analytical and Biological Aspects*, ed. P. Hänninen and H. Härmä, Springer Berlin Heidelberg, Berlin, Heidelberg, 2011, pp. 1–45. DOI: 10.1007/4243_2010_3.
11 S. I. Weissman, *J. Chem. Phys.*, 1942, **10**, 214–217.
12 A. P. S. Samuel, J. Xu and K. N. Raymond, *Inorg. Chem.*, 2009, **48**, 687–698.
13 A. D'Aléo, F. Pointillart, L. Ouahab, C. Andraud and O. Maury, *Coord. Chem. Rev.*, 2012, **256**, 1604–1620.
14 D. Mouchel Dit Leguerrier, R. Barré, J. K. Molloy and F. Thomas, *Coord. Chem. Rev.*, 2021, **446**, 214133.
15 N. Kwon, D. Kim, K. M. K. Swamy and J. Yoon, *Coord. Chem. Rev.*, 2021, **427**, 213581.
16 Y. Xiao, R. Zhang, Z. Ye, Z. Dai, H. An and J. Yuan, *Anal. Chem.*, 2012, **84**, 10785–10792.
17 Y. Xiao, Z. Ye, G. Wang and J. Yuan, *Inorg. Chem.*, 2012, **51**, 2940–2946.
18 X. Liu, Z. Tang, B. Song, H. Ma and J. Yuan, *J. Mater. Chem. B*, 2017, **5**, 2849–2855.
19 Z. Wang, Y. Huang, B. Song, Y. Shi and J. Yuan, *Inorg. Chem.*, 2025, **64**, 8685–8693.
20 H. Ma, B. Song, Y. Wang, D. Cong, Y. Jiang and J. Yuan, *Chem. Sci.*, 2017, **8**, 150–159.
21 H. Ma, B. Song, Y. Wang, C. Liu, X. Wang and J. Yuan, *Dyes Pigm.*, 2017, **140**, 407–416.
22 E. Del Giorgio and T. J. Sørensen, *Molecules*, 2020, **25**, 1959.
23 A. Picot, A. D'Aléo, P. L. Baldeck, A. Grichine, A. Duperray, C. Andraud and O. Maury, *J. Am. Chem. Soc.*, 2008, **130**, 1532–1533.
24 N. Hamon, A. Roux, M. Beyler, J. C. Mulatier, C. Andraud, C. Nguyen, M. Maynadier, N. Bettache, A. Duperray, A. Grichine, S. Brasselet, M. Gary-Bobo, O. Maury and R. Tripier, *J. Am. Chem. Soc.*, 2020, **142**, 10184–10197.
25 K. P. Malikidogo, T. Charnay, D. Ndiaye, J. H. Choi, L. Bridou, B. Chartier, S. Erbek, G. Micouin, A. Banyasz, O. Maury, V. Martel-Frachet, A. Grichine and O. Sénèque, *Chem. Sci.*, 2024, **15**, 9694–9702.
26 D. Akl, L. Bridou, M. Hojorat, G. Micouin, S. R. Kiraev, F. Riobé, S. Denis-Quanquin, A. Banyasz and O. Maury, *Eur. J. Inorg. Chem.*, 2024, 27.
27 X. L. Armesto, M. Canle L, M. I. Fernández, M. V. García and J. A. Santaballa, *Tetrahedron*, 2000, **56**, 1103–1109.
28 V. Lebrun, J.-L. Ravanat, J.-M. Latour and O. Sénèque, *Chem. Sci.*, 2016, **7**, 5508–5516.
29 M. Le Fur, M. Beyler, E. Molnar, O. Fougere, D. Esteban-Gomez, G. Tircso, C. Platas-Iglesias, N. Lepareur, O. Rousseaux and R. Tripier, *Inorg. Chem.*, 2018, **57**, 2051–2063.
30 M. Le Fur, E. Molnar, M. Beyler, O. Fougere, D. Esteban-Gomez, O. Rousseaux, R. Tripier, G. Tircso and C. Platas-Iglesias, *Inorg. Chem.*, 2018, **57**, 6932–6945.
31 B. Chartier, N. Hamon, D. Akl, A. Sickinger, L. Corne, G. Micouin, A. Banyasz, O. Maury, S. Erbek, V. Martel-Frachet, A. Grichine, M. Beyler, O. Sénèque and R. Tripier, *Chem. – Eur. J.*, 2025, **31**, e02044.
32 A. T. Bui, A. Roux, A. Grichine, A. Duperray, C. Andraud and O. Maury, *Chem. – Eur. J.*, 2018, **24**, 3408–3412.
33 V. Lebrun, J.-L. Ravanat, J.-M. Latour and O. Sénèque, *Chem. Sci.*, 2016, **7**, 5508–5516.
34 The difference in the enhancement factor is explained by the initial emission spectra. $\mathbf{TbL_2}$ is almost non emissive and therefore the initial Tb emission intensity is very low, upon oxidation the Tb luminescence is restorered resulting in a more important enhancement factor.